Physicochem. Probl. Miner. Process., 57(2), 2021, 70-82

http://www.journalssystem.com/ppmp

Physicochemical Problems of Mineral Processing

ISSN 1643-1049

Received June 17, 2020; reviewed; accepted January 24, 2021

Improvement of leaching efficiency of cathode material of spent $LiNi_xCo_yMn_zO_2$ lithium-ion battery by the in-situ thermal reduction

Qichang Lu [1], Haidi Jiang [1], Weining Xie [2], Guangwen Zhang [3], Yaqun He [1], Chenlong Duan [1], Jing Zhang [4], Zhaoyi Yu [1]

[1] School of Chemical Engineering & Technology, China University of Mining and Technology, Xuzhou 221116, Jiangsu, China

[2] Advanced Analysis and Computation Center, China University of Mining and Technology, Xuzhou 221116, Jiangsu, China

[3] School of Environmental Science and Spatial Informatics, China University of Mining and Technology, Xuzhou, 221116, China

[4] Department of Computer Science, Emory University, Georgia 30322, USA

Corresponding author: aacc_xwn5718@cumt.edu.cn (Weining Xie)

Abstract: Green cars and electronic products consume lots of lithium-ion batteries (LIBs), and massive spent LIBs are yielded due to performance degradation. This paper provides an economical and environmentally friendly approach to recover valuable metals from cathode materials of the spent LIBs. It combines the in-situ thermal reduction (self-reduction by polyvinylidene fluoride (PVDF) and residual electrolyte in cathode material) and sulfuric acid leaching. Elements of high valent are reduced by the binder (PVDF) and the residual electrolyte on the surface of NCM($LiNi_xCo_yMn_{1-x-y}O_2$) material at high temperatures. Moreover, the changes in substance type, element valency, and contents of cathode materials reduced with various terminal temperatures and retention time are analyzed by X-ray diffraction (XRD) and X-ray photoelectron spectroscopy (XPS). Results show that the optimal terminal temperature for in-situ thermal reduction is 600 °C, and the optimum retention time is 120 min. Under the best in-situ thermal reduction conditions, the results from XRD confirm that part of Ni^{2+} is converted to simple substance Ni, Co^{3+} is reduced to Co, and Mn^{4+} is reduced to Mn^{2+} and elemental Mn, which are confirmed by XRD. Analyzed results by XPS indicate that the content of Ni^{2+} decreases to 67.05%, and Co^{3+} is completely reduced to Co. Mn^{4+} is reduced to 91.41% of Mn^{2+} and 8.59% of simple substance Mn. In-situ thermal reduction benefits the leaching processes of cathode materials. The leaching efficiencies of Ni, Co, and Mn increase from 53.39%, 51.95%, and 0.71% to 99.04%, 96.98%, and 97.52%, respectively.

Keywords: spent lithium-ion batteries, in-situ thermal reduction, leaching efficiency, $LiNi_xCo_yMn_zO_2$

1. Introduction

The demand for lithium-ion batteries (LIBs) has grown dramatically due to the rapid development of electric vehicles and energy storage technologies, which now account for the largest share (Zhang et al., 2016). LIBs are typically used as power supplies since the advantages of high energy density and low self-discharge rate are obvious (Gao et al., 2018). However, the service life of LIB is limited, and statistics shows that there will be 500,000 tons of spent LIBs by 2020 (Liu et al., 2019, Golmohammadzadeh et al., 2018). With the continuous development of technology and industrial economy, the demand of metals increases dramatically (Afum et al., 2019). Valuable metals in spent LIBs include Li, Ni, Co, Mn, Cu, Fe, Al, etc (Zeng and Li, 2014b), and the grade is higher than that of natural ores (Zhu et al., 2020a). While toxic heavy metal substances and corrosive electrolytes in spent LIBs show the potential risks of environment pollution if they are not handled properly (Yang et al., 2016; Zhu et al., 2020b; Fu et al.,

DOI: 10.37190/ppmp/132762

2019). Therefore, it is essential to find methods for the effective and environmentally friendly recovery of spent LIBs. At present, standard methods are mainly hydrometallurgy, pyrometallurgy, and the combination of two ways (Barik et al., 2016). Among them, hydrometallurgy is widely applied because of the high metal recovery rate and low environmental impact. Hydrometallurgy mainly refers to the leaching by inorganic acid (Meshram et al., 2015). Chemical bonds of cathode materials are destroyed during the acid leaching process, and valuable metals are in solution with the ion form. However, the leaching process with organic acid or inorganic acid faces the following two problems:

Generally, the organic binder (such as PVDF) is used to adhere cathode material to aluminum sheet (Gratz et al., 2014). It makes the surface of all cathode materials covered by the organic film, which make it difficult for cathode materials falling off from the correct collector. It results in a negative effect on the leaching process. So, the first problem is how to effectively remove binder (PVDF) and other organic matter effectively. Wang et al. used a low-temperature roasting method. The optimal removal of the organic layer and the original exposed surface of cathode material were achieved under the calcination condition at 450 ℃ for 15 min (Wang et al., 2018). Zhang et al. put the mixture of electrode material and current collector into a water bath at 55 ℃, and the separation of two types of materials was realized by the combination of ultrasonic and stirring (Zhang et al., 2014). Except for the methods above, the separation of electrode material from the current collector can be achieved by dissolving the binder in solvent (He et al., 2017; He et al., 2018). Lu et al. placed the electrode sheet in N-methyl pyrrolidone (NMP) to dissolve the binder and realize the separation of cathode material from Al sheet (Yao et al., 2015). The current collector also can be dissolved by an alkali solution. Ferreira et al. dissolved spent cathode sheet with 10% (in mass) NaOH, followed by the twice leaching processes in solid-liquid ratio at 1:30 g/cm^3, temperature 30 ℃ and time 1 h. Nearly 80% Al was removed (Ferreira et al., 2009).

On the other hand, due to the existence of strong chemical bonds and high-valence elements, the leaching efficiency of the cathode material cannot reach the optimal value even under a long leaching time. Therefore, many studies focused on the reduction of metal by adding the reducing agent hydrogen peroxide (H_2O_2) at the leaching stage. Meshram et al. studied the leaching treatment of waste LIBs cathode materials treated by sulfuric acid. Under the best conditions (1 M H_2SO_4 at 368 K and 50 g/dm^3 pulp density for 240 min), the leaching rates of Li, Ni, Co, and Mn are 93.4%, 96.3%, 66.2%, and 50.2%, respectively. He found that the poor leaching efficiency is caused by the organic film on the surface of cathode materials. To improve the leaching efficiency, it is necessary to add a reducing agent (such as H_2O_2) (Meshram et al., 2015). Also, reducing materials were added with cathode for a thermal reduction before leaching. Liu et al. mixed the spent NCM($LiNi_xCo_yMn_zO_2$) with coke for vacuum pyrolysis, followed by water leaching and sulfuric acid leaching. Under the conditions of calcination temperature of 650 ℃, coke content of 10% , and calcination time of 30 min, the leaching efficiencies of Li, Ni, Co, and Mn were 93.67%, 93.33%, 98.08% and 98.68%, respectively (Liu et al., 2019). Zhang et al. conducted the leaching of treated spent NCM, which was thermally reduced by lignite. Under the conditions of calcination temperature of 650 ℃, lignite content of 20% and calcination time of 3 h, the leaching efficiency of Li was more than 80%, and leaching efficiencies of Ni, Co, and Mn were more than 96% (Zhang, J. et al., 2018). In summary, the methods above show some inevitable shortcomings for the separation of cathode material with current collector and destruction of strong chemical bond for the higher leaching efficiency of metal. For example, the addition of reducing reagents (except H_2O_2) in thermal or leaching treatment would result in the introduction of impurities.

The cathode plate of one LIB generally consists of the cathode material ($LiCoO_2$, $LiNi_xCo_yMn_zO_2$, and $LiFePO_4$), conductive agent (acetylene black), binder (PVDF), and current collector of Al sheet (Yao et al., 2018). The organic film composed of the PVDF and the electrolyte covers all gains of cathode material. All organic components have a certain degree of reducibility. Therefore, the binder (PVDF) and other organic substances on the spent cathode can be used as reducing agent to perform thermal reduction under anaerobic conditions. The composition and structure of cathode sheet used in this experiment is shown in Fig. 1. This paper uses the spent cathode of NCM as experimental materials, and the in-situ thermal reduction tests are conducted under various conditions. Then, XRD and XPS are used to analyze changes in substance type, and valency, and content of elements before and after the thermal reduction. Finally, effects of experimental conditions, namely terminal temperature and

retention time, on thermal reduction results are further investigated by sulfuric acid leaching tests with the same condition.

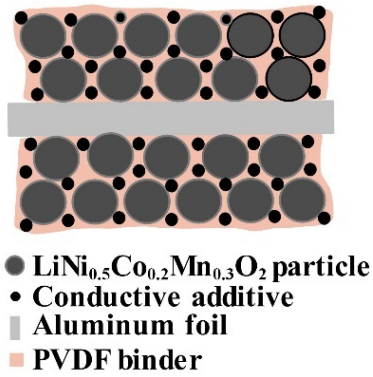

Fig. 1. Schematic diagram of the composition and structure of the cathode sheet

2. Experimental

2.1. Materials and reagents

Samples used in this research were spent LIBs of 18650(A standard lithium-ion battery model set by the Japanese company SONY, where 18 indicates a diameter of 18 mm, 65 indicates a length of 65 mm, and 0 indicates a cylindrical battery.). First, spent LIBs were immersed in 5wt % sodium chloride solution for 24 h for discharge treatment, and dried naturally. Then, spent LIBs were manually disassembled to obtain the cathode sheet. The size of the cathode sheet used in the in-situ thermal reduction experiment was 10 cm in length and 5 cm in width, and the mass of each sheet was 5 g. The content of each element in the spent NCM was measured by inductively coupled plasma mass spectrometry (ICP-MS), and results are shown in Table 1. Then, mass ratios among elements were converted to number ratios of atoms, and the NCM material was confirmed as $LiNi_{0.5}Co_{0.2}Mn_{0.3}O_2$(NCM523). The binder of the cathode and other organic substances were used as reducing substances for in-situ thermal reduction. Then the valuable metal elements are leached with sulfuric acid.

Table1. Main components of waste cathode materials

Element	Li	Ni	Co	Mn
Mass content/ %	7.86	34.38	13.38	16.94

2.2. Measurement and characterization

In-situ thermal reduction experiments were conducted in a tube furnace with the controlled atmosphere (MXG1200-80, Shanghai Micro-X Furnace). Pyrolysis properties of cathode materials were analyzed by the thermogravimetric analysis method (TG, Netzsch STA 449 F5, Germany). Phase characteristics and substance type of spent NCM before and after the in-situ thermal reduction were analyzed by X-ray diffractometer (XRD, Bruker D8 Advance, Germany). Changes in valency state and content of elements in various states were analyzed by X-ray photoelectron spectroscopy (XPS, Thermo Fisher Escalab 250Xi, America). ICP-MS measured concentrations of Ni, Co, and Mn in the leaching solution, and the leaching efficiency of each element was calculated.

2.3. Experimental process

2.3.1. Feasibility study of thermal reduction

The disassembled cathode sheet was placed in a vacuum tube furnace and subjected to thermal reduction under air and nitrogen conditions respectively (heating rate of 10℃/min, thermal reduction temperature of 600 ℃, nitrogen and air flow rate of 200 cm^3/min, the thermal reduction retention time of 120 min). The cathode sheet after the in-situ thermal reduction treatment is crushed and sieved to

obtain -0.074 mm NCM material, which is then tested by XRD and XPS to compare the phase and valence changes of each element.

2.3.2. Thermal reduction process under various terminal temperature and retention times

Pyrolysis characteristics of cathode material derived from spent LIBs were respectively analyzed using a thermogravimetric analyzer (NETZSCH, STA 449-F5, Germany, testing condition: temperature rises from 30 ℃ to 700 ℃ with heating rate of 10℃/min; N2 was used as shielding gas with an airflow velocity of 20 cm^3/min). For the in-situ thermal reduction tests, cathode sheet was introduced into a cold furnace and heated up then. Cathode sheet was in-situ thermal reduced at different temperature (450 ℃, 500 ℃, 550 ℃, 600 ℃) for the retention time of 120 min in a vacuum tube furnace under a nitrogen atmosphere to confirm the optimum thermal reduction temperature. At the optimum temperature, retention time (0 min, 15 min, 30 min, 60 min, 120 min) was changed to achieve the best thermal reduction.

2.3.3. Acid leaching tests of reduced materials under various conditions

Reduced products treated by various conditions and raw materials were subjected to the sulfuric acid leaching. Experimental conditions of leaching were: sulfuric acid concentration of 4 mol/dm^3, leaching temperature of 85 ℃, leaching time of 60 min, stirring speed of 300 rpm, and solid-liquid ratio of 0.1 g/cm^3. The leachate was subjected to ICP-MS to measure concentrations of Ni, Co, and Mn, and the leaching efficiency was calculated as follows:

$$E_i = \frac{c_i v_i}{m_i \omega_i} \times 100\% \quad (1)$$

where Ei represents the leaching efficiency of Ni, Co, Mn elements, ci is the concentration of metal ions in the leaching solution (g/dm^3), vi represents the volume of the leaching solution (dm^3), mi is the mass of the spent NCM523 (g), wi represents the content of the metal ions in the spent NCM523 (%).

3. Results and discussion

3.1. Pyrolysis characteristics of cathode material

The thermal decomposition behavior of cathode material was analyzed with thermogravimetric analysis and the TG and DTG curves are shown in Fig. 2. It can be seen that the weight loss process of cathode material is mainly divided into three stages, the first stage is 30 ℃-150 ℃ with the weight loss rate of 0.63%; the second stage is 150 ℃-350 ℃ with the weight loss rate of 1.37%; the third stage is 350 ℃-600 ℃, and the weight loss rate is 1.60%. The initial mass of cathode material in the TG test is 20.50 mg, the mass is reduced by 0.55 mg, 0.64 mg, 0.70 mg, and 0.73 mg at 450 ℃, 500 ℃, 550 ℃, and 600 ℃, respectively. So, the organic content in the cathode material is about 3.56%.

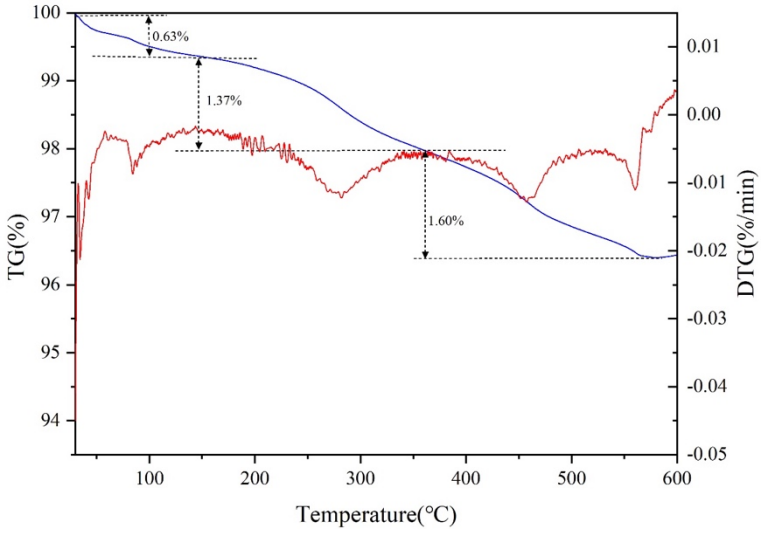

Fig. 2. TG and DTG analysis of the cathode material

3.2. Feasibility analysis of in-situ thermal reduction

XRD spectrums of the spent NCM523 before and after the thermal reduction treatment under air and nitrogen atmosphere are shown in Fig. 3. These results show that only peaks of $LiNi_xCo_yMn_zO_2$ exist in the raw spent NCM523, which indicates that Ni, Co, and Mn are in the steady layered structure of cathode material. Also, these elements are still in the high valency. This figure demonstrates that the products of the spent NCM523 treated in air exhibit the similar spectrum pattern if compared with that of raw materials. Hence, it can be concluded that the chemical valency of elements do not change. The binder and other organic substances attached to the cathode material burn directly (Wang et al., 2018) and do not react with the cathode material. The XRD result of materials after the thermal reduction under anaerobic condition indicates the change of layered structure, with the yield of new substance and valency decrease of elements. Part of Ni^{2+} is reduced to simple substances, and the other is in +2 valence form. Co^{3+} is produced to simple substances Co, and Mn^{4+} is changed to Mn^{2+}.

To further characterize the effect of organic substances on the valency reduction of elements in NCM523 after the thermal reduction in anaerobic, narrow scanning of Ni, Co, and Mn were analyzed by XPS. The split peak fitting results of these three elements are described in Fig. 4, and the first figure indicates that the spent NCM523 and material after thermal treatment in air are in the form of Ni^{2+} at binding energies of $Ni2p_{1/2}$ and $Ni2p_{3/2}$. However, the elemental Ni is produced after the thermal reduction under anaerobic condition. As shown in Fig. 4(b), the spent NCM523 and material after thermal treatment in the air are present in the form of Co^{3+} at binding energies of $Co2p_{1/2}$ and $Co2p_{3/2}$. Nevertheless, for the thermal reduction under N_2, Co^{3+} is reduced to elemental Co. Similarly, in Fig. 4(c), the valency of Mn is reduced from +4 to +2 at the binding energy of $Mn2p_{1/2}$ and $Mn2p_{3/2}$ after the thermal reduction under anaerobic condition. Moreover, a small amount of elemental Mn is produced.

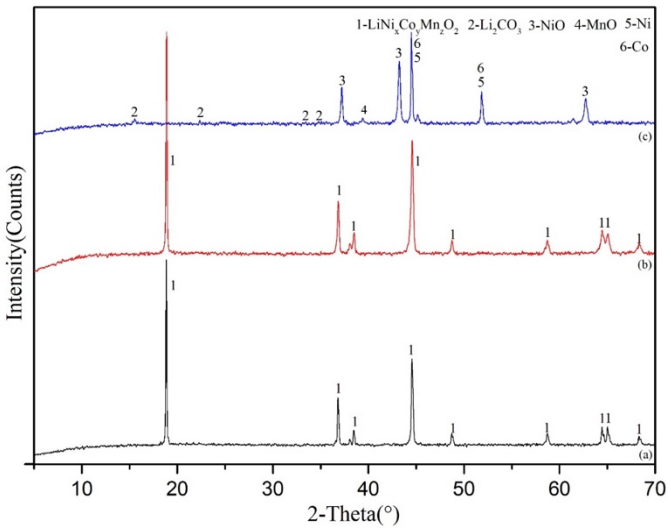

Fig. 3. (a)XRD spectrums of spent NCM523, (b) XRD spectrum of spent NCM523 after heat treatment in air at 600°C, 120min, (c) XRD spectrum of spent NCM523 after heat treatment in nitrogen at 600°C, 120min

In summary, the valencies of Ni, Co, and Mn do not change during thermal treatment under air condition, which indicates the same substance type with the raw spent NCM523. Organic films on the surface of NCM523 are oxidized and burned during the thermal treatment process, without interaction with NCM523. In the thermal reduction of anaerobic condition, the high-valency element is reduced to the low-valent form. Therefore, organic substances in cathode material can result in the in-situ thermal reduction in anaerobic condition, with the destruction of original structure of NCM523 and reduction of element valency.

3.3. Effect of terminal temperature and retention time on the in-situ thermal reduction

Previous exploration has verified the feasibility of thermal reduction of NCM523 by the attached binder and organic substances. As the terminal temperature has an essential effect on the reduction result, thermal reduction tests are designed with the terminal temperature of 450 °C, 500 °C, 550 °C, and 600 °C,

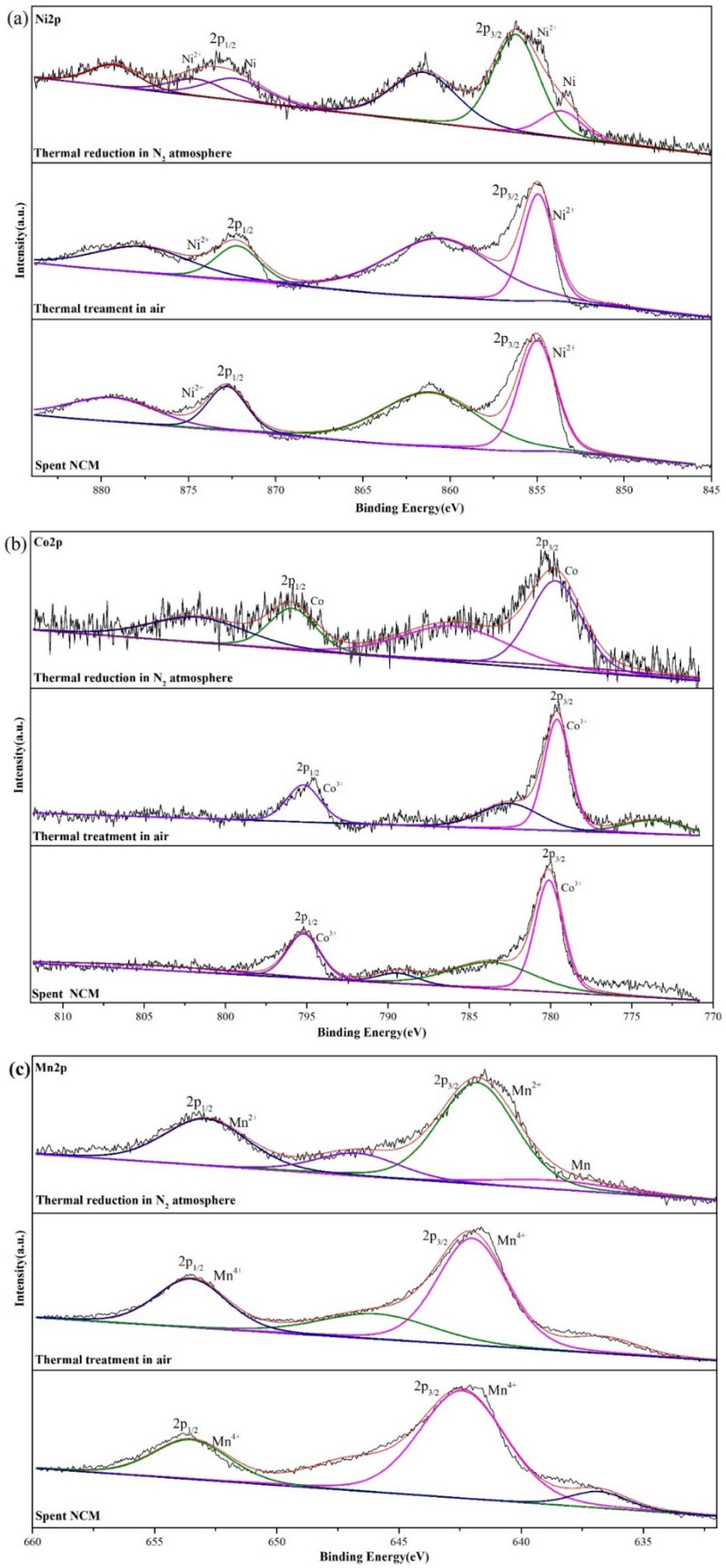

Fig. 4. Comparison of chemical valency of (a) Ni2p, (b) Co2p, and (c) Mn2p by XPS narrow scan data of spent NCM523, and spent NCM523 heat treatment in air and nitrogen at 600℃, 120min

and retention time is fixed for 2 h. Fig. 5 shows the XRD results date of spent NCM523 before and after the thermal reduction under various temperatures. Compared with the untreated material, the spent NCM523 treated at 450 ℃ and 500 ℃ for 120 minutes remains substantially unchanged. When the terminal temperature rises to 550 ℃, the $LiNi_xCo_yMn_zO_2$ decomposes as Li_2CO_3, NiO, MnO, elemental Ni and Co. This indicates that the reduction reaction has occurred. With the further increase of the terminal temperature, peaks of new substances decomposed from peaks of $LiNi_xCo_yMn_zO_2$ after the thermal reduction is pronounced, which means that the reduction reaction proceeds more thoroughly. Hence, the element valency decreases, with the generation of elemental Ni and Co, and MnO. Table2 depicts the contents of element Ni, Co and Mn of various valencies in spent NCM523 before and after the thermal reduction at different temperatures. With the terminal temperature levels as 450 ℃ and 500 ℃, the element valency and the content of each element stay the same. For the thermal reduction treatment at 550℃, 22.59% of Ni^{2+} is reduced to elemental Ni, 30.97% of Co^{2+} is reduced to elemental Co, and the content of Mn^{4+} decreases by 77.77%. When the temperature rises to 600 ℃, the content of elemental Ni increases to 32.95% and all Co^{3+} is reduced to elemental Co. Mn^{4+} is almost completely reduced to Mn^{2+}, and only 8.59% of elemental Mn is produced. The conclusions above are consistent with the analysis results of the XRD diffraction pattern except of elemental Mn presence, because the content of elemental Mn is low and is not found in the XRD diffraction pattern.

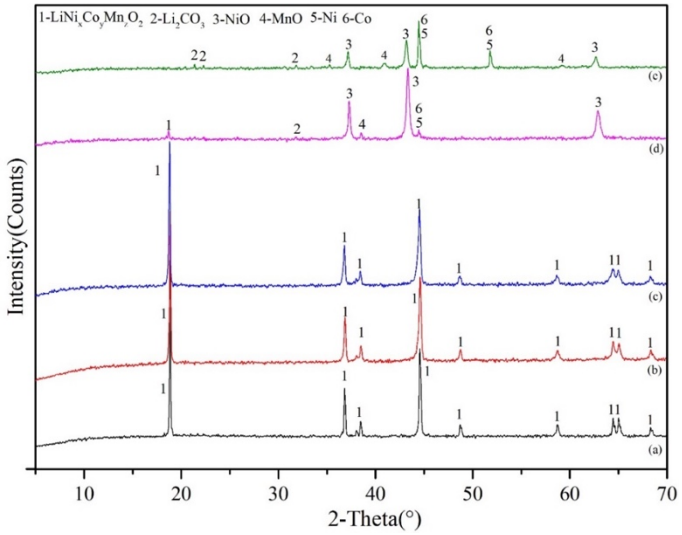

Fig. 5. (a) XRD diffraction pattern of spent NCM523, (b-e) XRD diffraction pattern of spent NCM523 after thermal reduction at 450 ℃, 500 ℃, 550 ℃ and 600 ℃ for 120 min in nitrogen

Table 2. Contents of elements of various valencies in spent NCM523 before and after the thermal reduction at various temperatures

Sample	Mass content/%						
	Ni^{2+}	Ni	Co^{3+}	Co	Mn^{4+}	Mn^{2+}	Mn
Spent NCM	100.00	0.00	100.00	0.00	100.00	0.00	0.00
450℃	100.00	0.00	100.00	0.00	100.00	0.00	0.00
500℃	100.00	0.00	100.00	0.00	100.00	0.00	0.00
550℃	77.41	22.59	69.03	30.97	22.23	77.77	0.00
600℃	69.05	30.95	0.00	100.00	0.00	91.41	8.59

Besides the terminal temperature, the retention time also influences the thermal reduction result. Fig. 5 describes the XRD results of raw spent NCM523, and products reduced in various retention times (0 min, 15 min, 30 min, 60 min, and 120 min) at 600 ℃. It should be noted that the thermal reduction test of retention time of 0 min undergoes the same heating-up process and materials are removed out after the terminal temperature of 600 ℃ is reached. The curves in Fig. 6 illustrate that the spent NCM523 with the retention time of 0 min has the same substance type as that of the untreated one. When the retention

time is 15 min, the layered structure starts to change, and the element valency is initially reduced. This demonstrates that the thermal reduction reaction mainly occurs within the constant temperature stage, and there is no noticeable change for the substance type during the heating-up process of 600 ℃. Table 3 shows the contents of elements of various valencies in the spent NCM523 after the thermal reduction treatment at different retention times of terminal temperature. Elemental Ni is produced at the retention time of 15 min, and its content increases from 18.62% at 15 min to 32.95% at 120 min. For the element Co, if the retention time is 15 min, Co^{3+} is reduced to Co^{2+} of 75.01% and elemental Co of 24.99%. As the retention time increases, Co^{3+} is finally reduced to elemental Co at the retention time of 120 min. 64.37% of Mn^{4+} is reduced to Mn^{2+} when the retention time at 600℃ is 15 min. With the increase of retention time, the content of Mn^{4+} decreases gradually. At 120 min, Mn^{4+} is finally reduced to Mn^{2+} of 91.41% and elemental Mn of 8.59%. The changes of the valencies in elements Ni, Co, and Mn under different retention times also confirm the variation of substance type.

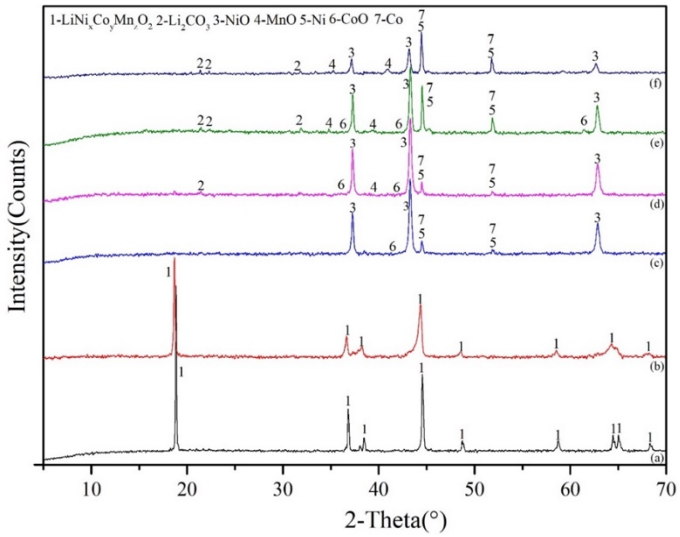

Fig. 6. XRD diffractogram of (a) untreated spent NCM523 and products after thermal reduction at 600 °C for different times (b) 0 min, (c) 15 min, (d) 30 min, (e) 60 min, (f) 120 min

Table 3. Contents of elements of various valencies in spent NCM 523 after thermal reduction at different retention times of 600℃

Sample	Mass content/%							
	Ni^{2+}	Ni	Co^{3+}	Co^{2+}	Co	Mn^{4+}	Mn^{2+}	Mn
0min	100.00	0.00	100.00	0.00	0.00	100.00	0.00	0.00
15min	81.38	18.62	0.00	75.01	24.99	35.63	64.37	0.00
30min	79.27	20.73	0.00	74.11	25.89	30.68	69.32	0.00
60min	68.74	31.26	0.00	55.17	44.83	28.58	71.42	0.00
120min	67.05	32.95	0.00	0.00	100.00	0.00	91.41	8.59

3.4. Analysis of the reaction of electrode materials during thermal reduction

The pyrolysis characteristics of the organic binder in the electrode material are shown in the analysis of potential chemical reactions. The first is the pyrolysis process of the organic binder PVDF. This process occurs between 450-550℃. PVDF decomposes into HF and pyrolysis residual carbon and various fluorobenzenes (as shown in chemical equation (2)). Secondly, due to the certain reduction characteristics of HF gas, part of $LiNi_{0.5}Co_{0.2}Mn_{0.3}O_2$ can be reduced to NiO, Co, MnO and LiF at 600°C (as shown in chemical equation (3)). At the same time, pyrolysis residual carbon and conductive agent can also reduce LiNi0.5Co0.2Mn0.3O2 to CoO and Li2O. Finally, NiO reacts with residual carbon to form Ni elemental substance (as shown in chemical equation (4)).

$$-(CF2CH2)-_n \rightarrow HF\uparrow + C(\text{Pyrolysis residual carbon}) + R(\text{Fluorobenzene}) \quad (2)$$

$$12HF + 5LiNi_{0.5}Co_{0.2}Mn_{0.3}O_2 = 2.5NiO + Co + 1.5MnO + 5LiF + 6H_2O + 3.5F_2 \uparrow \quad (3)$$

$$1.75C + 5LiNi_{0.5}Co_{0.2}Mn_{0.3}O_2 = 2.5Li_2O + 2.5NiO + Co + 1.5MnO + 1.75CO_2 \uparrow \quad (4)$$

$$2NiO + C = 2Ni + CO_2 \uparrow \quad (5)$$

3.5. Leaching experiments of thermal reduction products

Except for the discussion of thermal reduction results by instrumental analyses, products of various thermal reduction conditions are subjected to sulfuric acid leaching tests with the same experimental parameters (H_2SO_4 concentration of 4 mol/dm^3, leaching temperature of 85 °C, leaching time 60 min, stirring speed of 300 rpm, solid-liquid ratio of 0.1 g/cm^3). Table 4 shows the leaching efficiencies of Ni, Co, and Mn in raw spent NCM523 and materials after thermal reduction at various terminal temperatures for 120 min. To estimate the experimental error, this paper conducted repeat tests. The leaching tests of samples for each terminal temperature were repeated three times. The 95% confidence interval is the mean value of ±95% confidence limit. This table indicates that nearly all the experimental values are in the 95% confidence interval range. Meanwhile, the 95% confidence limit is 10% of the mean value (confidence limits are based on standard deviation). The relatively high repeatability of experimental data illustrates the validity of leaching tests. Fig. 7 shows the change trend of the leaching efficiency of Ni, Co and Mn in the raw spent NCM523 and the thermally reduced NCM material after the in-situ thermal reduction for 120 minutes at different terminal temperatures. Leaching efficiencies of Ni, Co, and Mn increase with the increase of terminal temperature (temperature for the in-situ thermal reduction tests). Organic materials such as binder are decomposed at those temperatures, and the surface of spent NCM523 is exposed, which benefits the leaching process (Zhang, G. et al., 2018). That is also why the leaching efficiencies of the treated spent NCM523 at low terminal temperature (450 °C and 500 °C) are higher than those of the raw one. For the high-temperature range (550 °C and 600 °C), the in-situ thermal reduction reaction caused by decomposition products of organic substances breaks the layered structure of $LiNi_xCo_yMn_zO_2$ and promotes the decrease of element valency. For the in-situ thermal reduction of high terminal temperature, chemical bond energies among elements become weak, and elements of low valency are easy to be leached in the acid solution. The change of leaching efficiency is more obvious for Mn of NCM523 treated at 550 °C and 600 °C than those of others. For the thermal reduction test at 600 °C, each element's leaching efficiency is the highest, and the average value of leaching efficiencies of Ni, Co and temperature of in-situ thermal reduction is 600 °C.

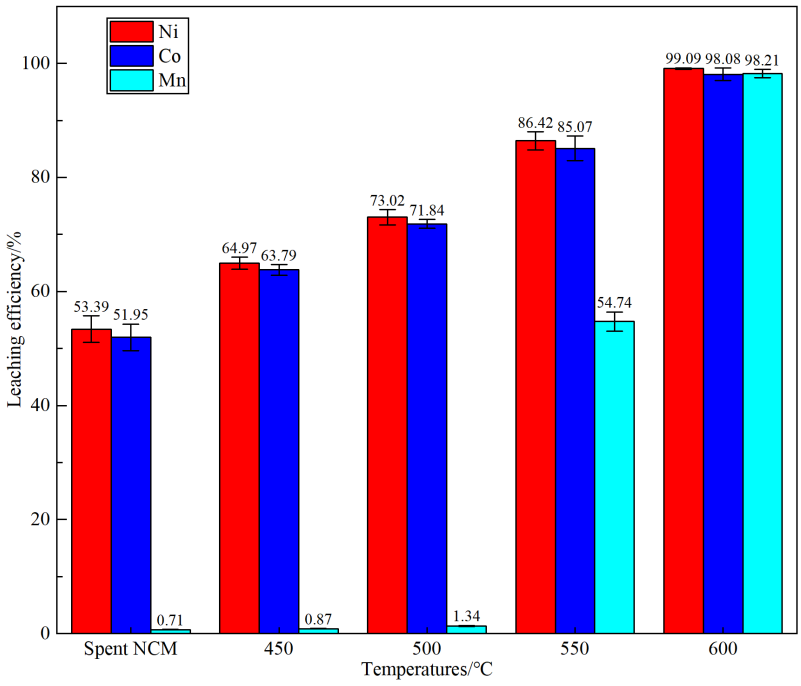

Fig. 7. Leaching efficiencies of Ni, Co and Mn elements of raw spent NCM523 and cathode material after the in-situ thermal reduction for 120 minutes at different terminal temperatures

Table 4. Leaching efficiencies of elements of products treated at different temperatures and confidence analyses of repeat experiments

Temperature/ ℃	Element type	Leaching efficiency/ %				95% Confidence limit	95% Confidence limit to the mean
		Repeat1	Repeat2	Repeat3	Mean		
Spent NCM	Ni	56.02	51.70	52.46	53.39	3.69	6.92
	Co	54.63	50.22	50.99	51.95	3.77	7.26
	Mn	0.70	0.71	0.73	0.71	0.02	3.43
450	Ni	63.88	65.06	65.97	64.97	1.68	2.58
	Co	63.10	63.46	64.82	63.79	1.45	2.28
	Mn	0.86	0.89	0.85	0.87	0.03	4.02
500	Ni	71.61	74.27	73.19	73.02	2.14	2.94
	Co	71.73	72.66	71.13	71.84	1.23	1.72
	Mn	1.25	1.40	1.37	1.34	0.13	9.48
550	Ni	88.23	85.71	85.33	86.42	2.52	2.92
	Co	87.55	84.07	83.59	85.07	3.46	4.07
	Mn	53.02	56.35	54.86	54.74	2.67	4.88
600	Ni	99.23	99.04	99.01	99.09	0.19	0.19
	Co	99.15	96.98	98.10	98.08	1.73	1.77
	Mn	98.97	97.52	98.15	98.21	0.09	0.09

Table 5 shows each element's leaching efficiency under the thermal reduction temperature of 600 ℃ for 0 min, 15 min, 30 min, 60 min, and 120 min. To estimate the experimental error, this paper also conducted repeat tests. The leaching conditions are the same as before. The relatively high repeatability of experimental data in Table 5 illustrates the validity of leaching tests. Fig. 8 shows the change trend of the leaching efficiency of Ni, Co and Mn under the thermal reduction temperature of 600 ℃ for 0 min, 15 min, 30 min, 60 min, and 120 min. It can be seen from the figure that the error on the histogram representing the leaching efficiency of each element is still small, which further verifies the good repeat-

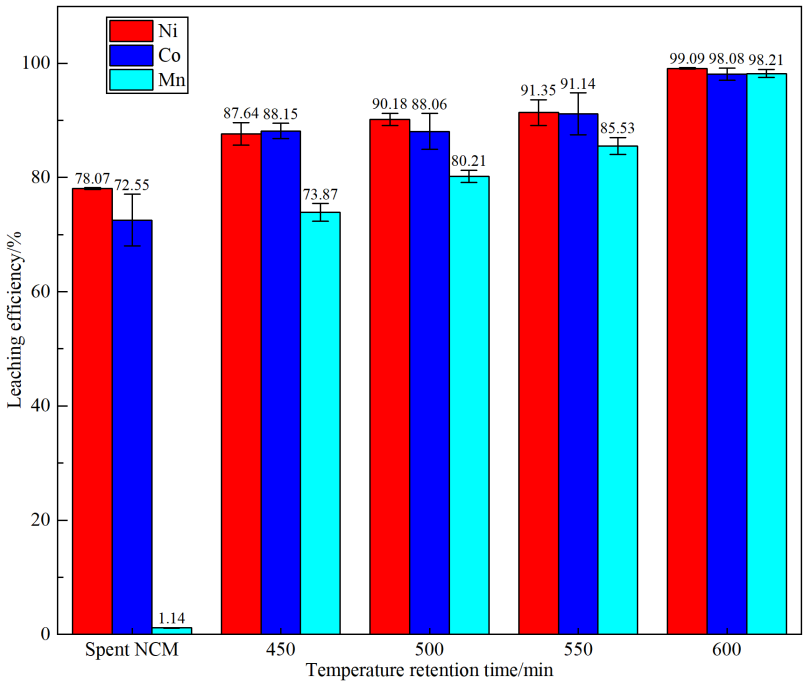

Fig. 8. Leaching efficiencies of Ni,Co and Mn elements of raw spent NCM523 and products treated at different temperature retention times

Table 5. Leaching efficiencies of elements of products treated at different temperature retention times of 600℃ and confidence analyses of repeat experiments.

Temperature retention time of 600℃/min	Element type	Leaching efficiency/%				95% Confidence limit	95% Confidence limit to the mean
		Repeat1	Repeat2	Repeat3	Mean		
0	Ni	78.23	77.93	78.06	78.07	0.24	0.31
	Co	77.78	69.94	69.92	72.55	7.25	10.00
	Mn	1.15	1.19	1.07	1.14	0.10	8.59
15	Ni	88.62	85.37	88.92	87.64	3.15	3.59
	Co	89.67	87.23	87.56	88.15	2.12	2.40
	Mn	72.52	75.57	73.51	73.87	2.49	3.38
30	Ni	91.10	89.01	90.44	90.18	1.71	1.90
	Co	91.46	87.44	85.28	88.06	5.02	5.70
	Mn	80.02	79.23	81.37	80.21	1.73	2.16
60	Ni	93.96	90.25	89.84	91.35	3.63	3.98
	Co	95.37	88.94	89.10	91.14	5.87	6.44
	Mn	87.15	84.30	85.15	85.53	2.34	2.74
120	Ni	99.23	99.04	99.01	99.09	0.19	0.19
	Co	99.15	96.98	98.10	98.08	1.73	1.77
	Mn	98.97	97.52	98.15	98.21	0.09	0.09

ability of the experiment. It should be noted that the longer retention time, the longer reduction reaction time. Hence, the content of elements with the reduction of valency increases. Results in Table 5 indicate that leaching efficiency of each element increases with the retention time. When the retention time is 120 minutes, the best results of in-situ thermal reduction are achieved, with the highest leaching efficiency. Another interesting result is that the leaching efficiencies of elements for the terminal temperature of 600℃ and retention time of 0 min are higher than those of low temperature (450 ℃ and 500 ℃) and retention time of 120 min. Since there is a 10min heating-up process from 500℃ to 600℃, some weak reduction reaction may occur during this process, and result in the valency decrease of part of elements.

4. Conclusions

A method of in-situ thermal reduction by the binder and other organic substances of the spent NCM523 in the nitrogen atmosphere is proposed to reduce the element valency for the improvement of leaching efficiency. Conclusions of this paper are as follows:

1. Exploratory experiments show that in the air atmosphere of 600 ℃, organic films on the surface of spent NCM523 burn directly. Valency of elements in cathode materials do not change. While under the nitrogen atmosphere, the in-situ thermal reduction reaction of the spent NCM523 occurs with the decrease of element valency (illustrated by XPS) and generation of new metal substances (analyzed by XRD).

2. For conditions of fixed retention time of terminal temperature, the higher terminal temperature can accelerate the process of the in-situ thermal reduction reaction, with the higher yield of the low-valency element. After the terminal reduction at 550 ℃, the original chemical bonds among elements of spent NCM523 are destroyed, and the element valency decreases. If the temperature further increases to 600 ℃, 32.95% of elemental Ni will be generated. All of Co^{3+} is reduced to elemental Co. Mn^{4+} is almost completely reduced to Mn^{2+}, and 8.59% of elemental Mn is yielded. With the increase of the terminal temperature, the leaching efficiencies of Ni, Co, and Mn increase with the decrease of element valency. Leaching efficiencies of all elements reach the highest at 600 ℃.

3. The retention time of the final temperature has a decisive influence on the in-situ thermal reduction process. Thermal reduction mainly occurs in the high-temperature section, and there is no

obvious change in the substance type during the heating-up process. If the retention time is 15 min, the layered structure will be destroyed, and element valency will be reduced. At this time, 18.62% of elemental Ni and 24.99% of elemental Co will be produced. While retention time increases to 120 min, reduction reaction proceeds more completely, and elements of Ni, Co, and Mn exist in a low-valent form. At the terminal temperature of 600 ℃ and retention time of 120min, the best thermal reduction results are achieved, and the leaching efficiencies of Ni, Co, and Mn also reach optimal values, which are 99.04%, 96.98% and 97.52%, respectively.

Acknowledgments

Works in this paper were supported by the National Natural Science Foundation of China (51904295), Science Foundation of Jiangsu province (BK20180647), Inner Mongolia Science & Technology Plan (2019GG274), and the Priority Academic Program Development of Jiangsu Higher Education Institutions. Authors are also thankful for the technical support of the Advanced Analysis & Computation Center and support by the Key-Area Research and Development Program of Guangdong Province（2020B090919003）, Special fund (Social Development) project of key research and development plan of Jiangsu Province (BE2019634).

References

AFUM, B.O., CAVERSON, D., BEN-AWUAH, E., 2019. *A conceptual framework for characterizing mineralized waste rocks as future resource*. International Journal of Mining Science and Technology 29(3), 429-435.

BARIK, S.P., PRABAHARAN, G., KUMAR, B., 2016. *An innovative approach to recover the metal values from spent lithium-ion batteries*. Waste Management 51, 222-226.

FERREIRA, D.A., ZIMMER PRADOS, L.M., MAJUSTE, D., MANSUR, M.B., 2009. *Hydrometallurgical separation of aluminium, cobalt, copper and lithium from spent Li-ion batteries*. Journal of Power Sources 187(1), 238-246.

FU, Y., HE, Y., CHEN, H., YE, C., LU, Q., LI, R.., 2019. *Effective leaching and extraction of valuable metals from electrode material of spent lithium-ion batteries using mixed organic acids leachant*. Journal of Industrial and Engineering Chemistry 79,154-162.

GAO, W., LIU, C., CAO, H., ZHENG, X., LIN, X., WANG, H., ZHANG, Y., SUN, Z., 2018. *Comprehensive evaluation on effective leaching of critical metals from spent lithium-ion batteries*. Waste Management 75, 477-485.

GOLMOHAMMADZADEH, R., FARAJI, F., RASHCHI, F., 2018. *Recovery of lithium and cobalt from spent lithium ion batteries (LIBs) using organic acids as leaching reagents: A review.* Resources Conservation and Recycling 136, 418-435.

GRATZ, E., SA, Q., APELIAN, D., WANG, Y., 2014. *A closed loop process for recycling spent lithium ion batteries.* Journal of Power Sources 262, 255-262.

HE, L.-P., SUN, S.-Y., SONG, X.-F., YU, J.-G., 2017. *Leaching process for recovering valuable metals from the* $LiNi_{1/3}Co_{1/3}Mn_{1/3}O_2$ *cathode of lithium-ion batteries*. Waste Management 64, 171-181.

HE, L.-P., SUN, S.-Y., YU, J.-G., 2018. *Performance of* $LiNi_{1/3}Co_{1/3}Mn_{1/3}O_2$ *prepared from spent lithium-ion batteries by a carbonate co-precipitation method*. Ceramics International 44(1), 351-357.

LIU, P., XIAO, L., TANG, Y., CHEN, Y., YE, L., ZHU, Y., 2019. *Study on the reduction roasting of spent LiNixCoyMnzO2 lithium-ion battery cathode materials*. J. Therm. Anal. Calorim. 136(3), 1323-1332.

MESHRAM, P., PANDEY, B.D., MANKHAND, T.R., 2015. *Recovery of valuable metals from cathodic active material of spent lithium ion batteries: Leaching and kinetic aspects*. Waste Management 45, 306-313.

MESHRAM, P., PANDEY, B., MANKHAND, T.J.C.E.J., 2015. *Hydrometallurgical processing of spent lithium ion batteries (LIBs) in the presence of a reducing agent with emphasis on kinetics of leaching*. Chemical Engineering Journal 281, 418-427.

WANG, F., ZHANG, T., HE, Y., ZHAO, Y., WANG, S., ZHANG, G., ZHANG, Y., FENG, Y., 2018. *Recovery of valuable materials from spent lithium-ion batteries by mechanical separation and thermal treatment*. Journal of Cleaner Production 185, 646-652.

YANG, Y., HUANG, G., XU, S., HE, Y., LIU, X., 2016. *Thermal treatment process for the recovery of valuable metals from spent lithium-ion batteries*. Hydrometallurgy 165, 390-396.

YAO, Y., ZHU, M., ZHAO, Z., TONG, B., FAN, Y., HUA, Z.J.A.S.C., 2018. *Hydrometallurgical processes for recycling spent lithium-ion batteries: a critical review.* ACS Sustainable Chemistry & Engineering 6,13611-13627.

YAO, L., FENG, Y., XI, G., 2015. *A new method for the synthesis of $LiNi_{1/3}Co_{1/3}Mn_{1/3}O_2$ from waste lithium ion batteries*. Rsc Advances 5(55), 44107-44114.

ZENG, X., LI, J., 2014. *Spent rechargeable lithium batteries in e-waste: composition and its implications*. Frontiers of Environmental Science & Engineering 8(5), 792-796.

ZHANG, G., HE, Y., FENG, Y., WANG, H., ZHANG, T., XIE, W., ZHU, X., 2018. *Enhancement in liberation of electrode materials derived from spent lithium-ion battery by pyrolysis*. Journal of cleaner production 199, 62-68.

ZHANG, J., HU, J., ZHANG, W., CHEN, Y., WANG, C., 2018. *Efficient and economical recovery of lithium, cobalt, nickel, manganese from cathode scrap of spent lithium-ion batteries*. Journal of cleaner production 204, 437-446.

ZHANG, T., HE, Y., WANG, F., GE, L., ZHU, X., LI, H., 2014. *Chemical and process mineralogical characterizations of spent lithium-ion batteries: An approach by multi-analytical techniques*. Waste Management 34(6), 1051-1058.

ZHANG, X., XUE, Q., LI, L., FAN, E., WU, F., CHEN, R., 2016. *Sustainable Recycling and Regeneration of Cathode Scraps from Industrial Production of Lithium-Ion Batteries*. Acs Sustainable Chemistry & Engineering 4(12), 7041-7049.

ZHU, X.-N., ZHANG, H., NIE, C.-C., LIU, X.-Y., LYU, X.-J., TAO, Y.-J., QIU, J., LI, L., ZHANG, G.-W., 2020a. *Recycling metals from-0.5 mm waste printed circuit boards by flotation technology assisted by ionic renewable collector*. Journal of Cleaner Production 258, 120628.

ZHU, X.-N., ZHANG, Y.-K., ZHANG, Y.-Q., YAN, Z.-Q., NIE, C.-C., LYU, X.-J., TAO, Y.-J., QIU, J., LI, L., 2020b. *Flotation dynamics of metal and non-metal components in waste printed circuit boards*. Journal of Hazardous Materials 392, 122322.